Electronic Supplementary Material (ESI) for Journal of Materials Chemistry C.

Supporting Information for

Highly Flexible Latex Photonic Films with Tunable Structural Colors Templated by Cellulose Nanocrystals

Junxiao Leng, Guihua Li, Xingxiang Ji, Zaiwu Yuan, Yingjuan Fu, Hongguang Li, Menghua Qin, Helmuth Moehwald

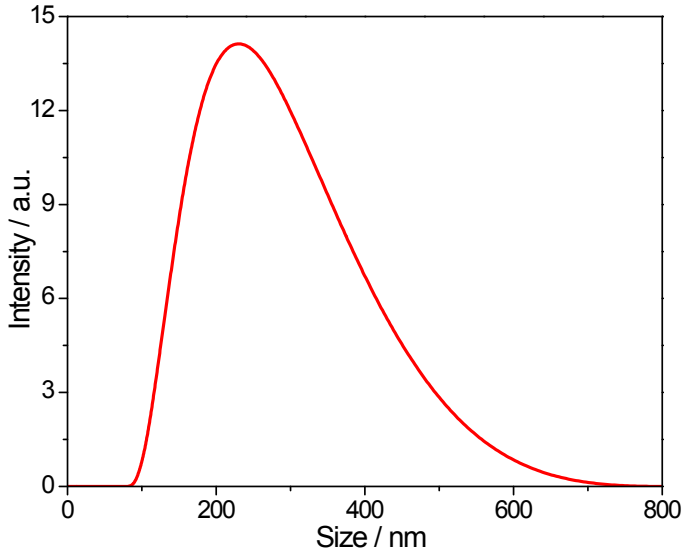

Fig. S1 Size distribution of SALs obtained from laser particle size analysis.

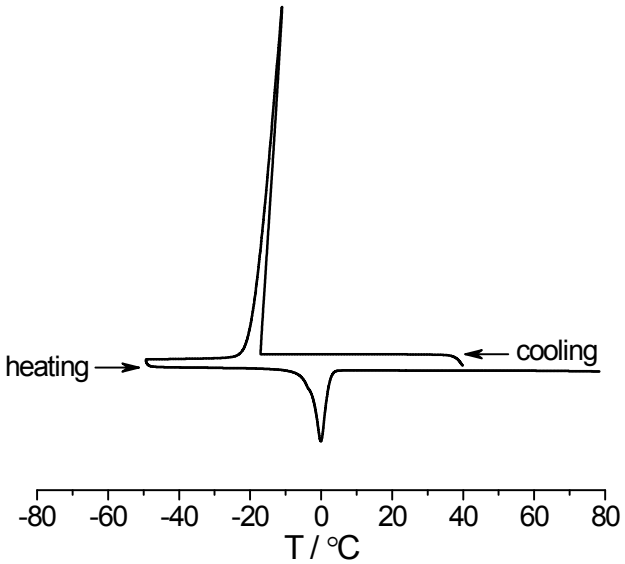

Fig. S2 DSC curve of the suspension of as-prepared SALs. The sharp peaks are caused by the crystalization of H_2O and melting of the ice.

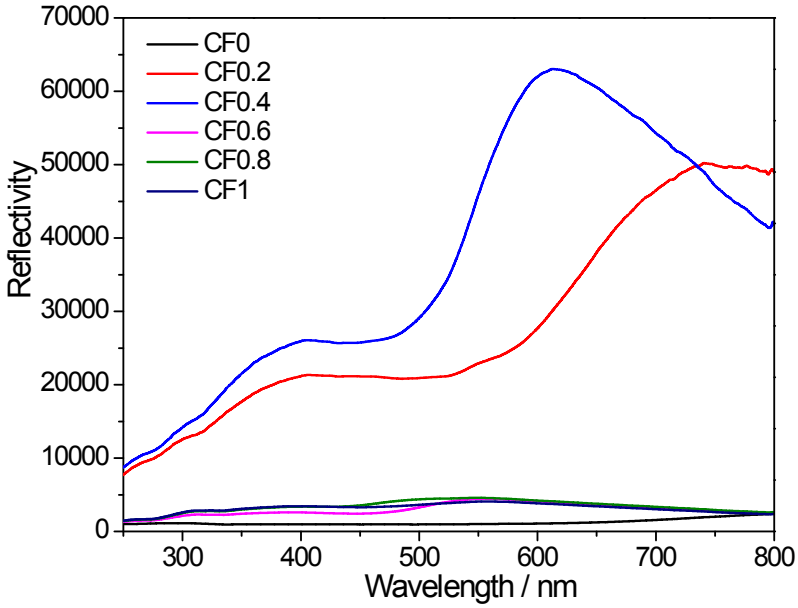

Fig. S3 Reflection spectra of CFs in the UV and visible region before normalization.

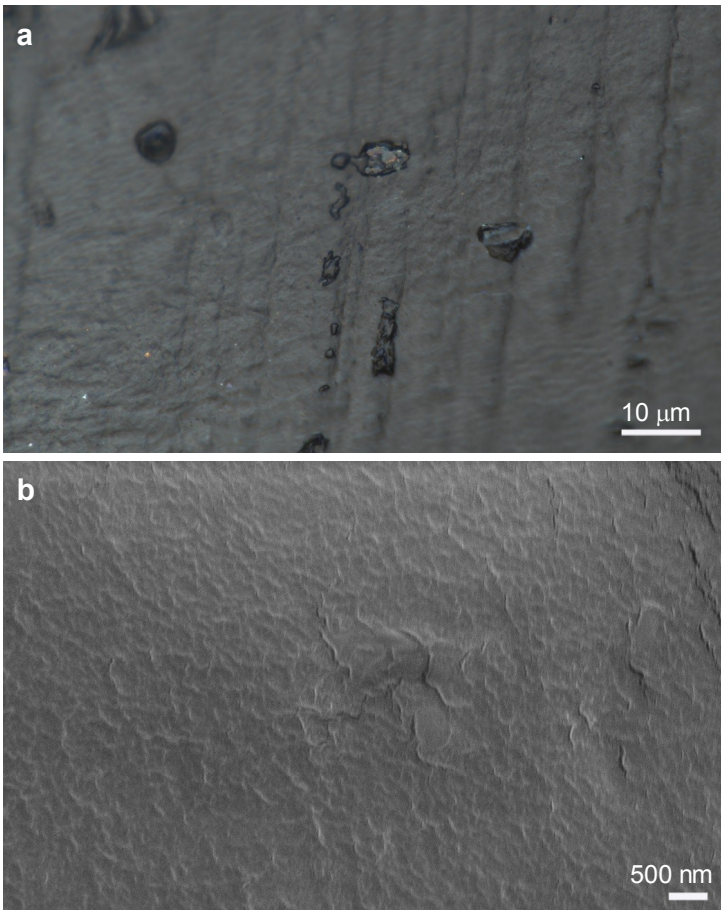

Fig. S4 a) POM image and b) SEM image of the fracture surface for the film formed solely by SALs.

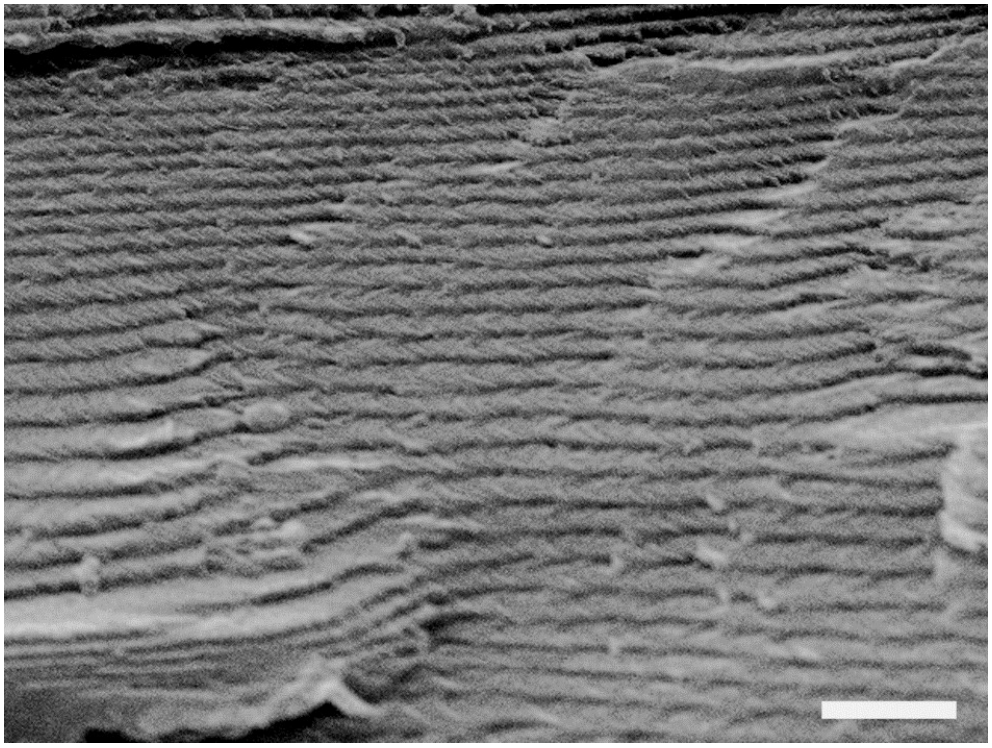

Fig. S5 SEM image at a higher magnification compared to that shown in the maintext (Fig. 3f) of the fracture surface of $CF_{0.4}$. The scale bar corresponds to 1 μm.

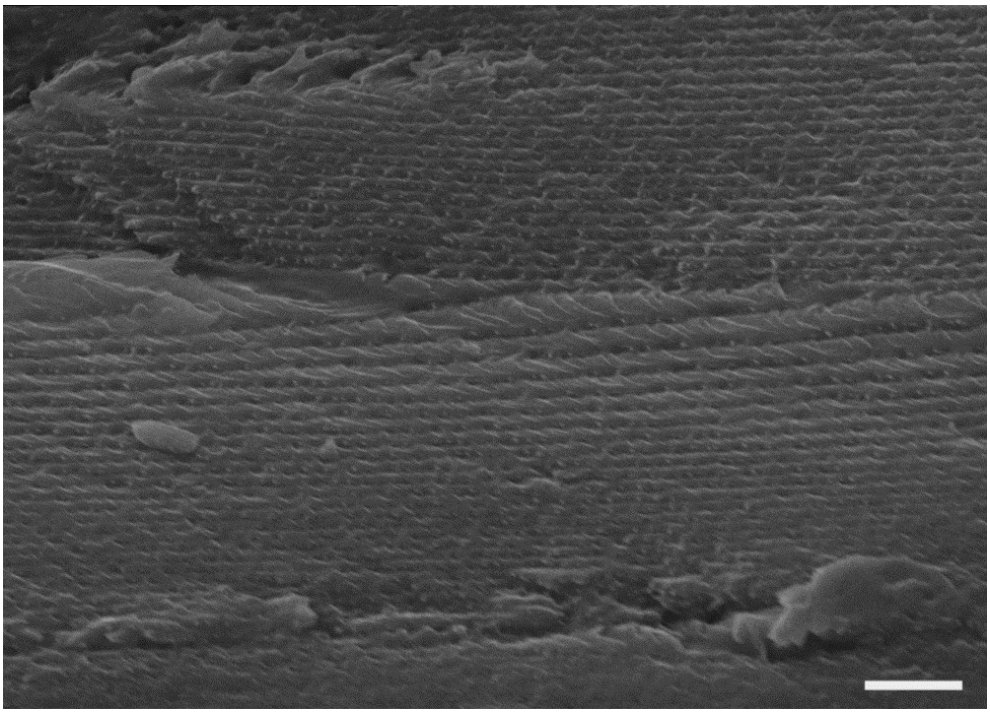

Fig. S6 A typical SEM image of the fracture surface of CF_0. The scale bar corresponds to 4 μm.

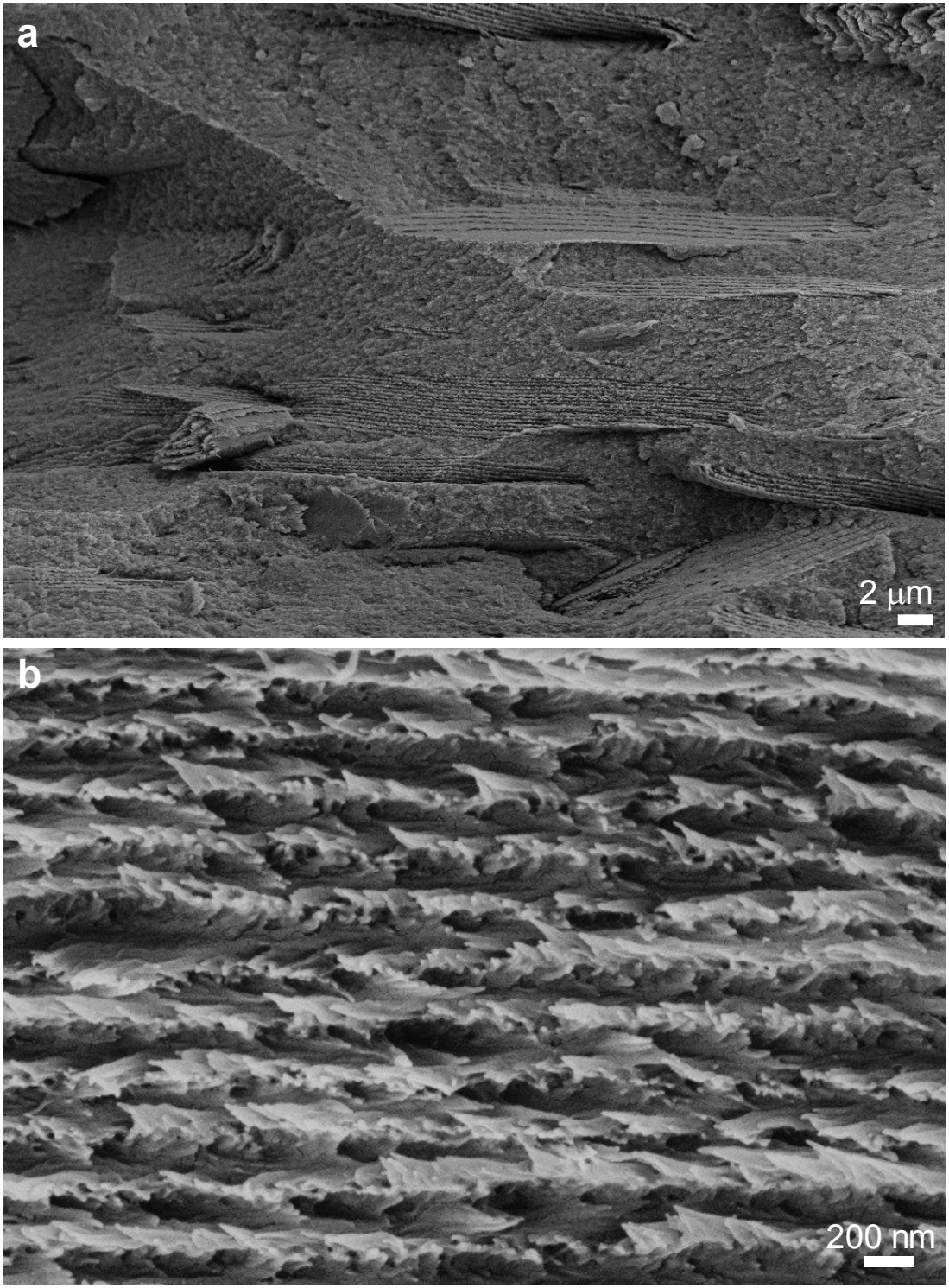

Fig. S7 a) SEM image at a lower magnification compared to that shown in the maintext (Fig. 3g) of $CF_{0.6}$. **b**) A magnified image focusing on the domain formed by CNCs.

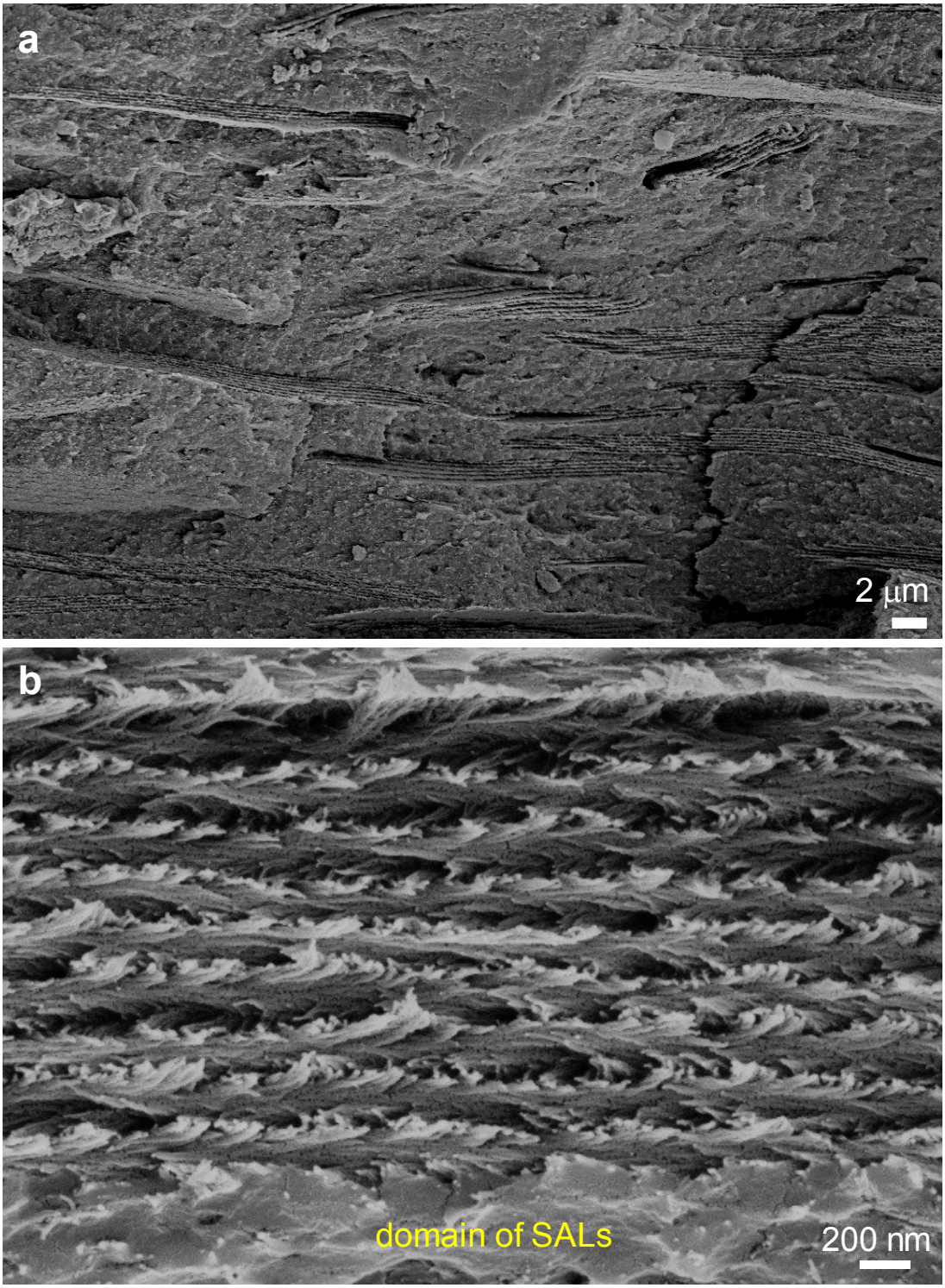

Fig. S8 a) SEM image at a lower magnification compared to that shown in the maintext (Fig. 3h) of $CF_{0.8}$. **b**) A magnified image focusing on the domain rich in CNCs.

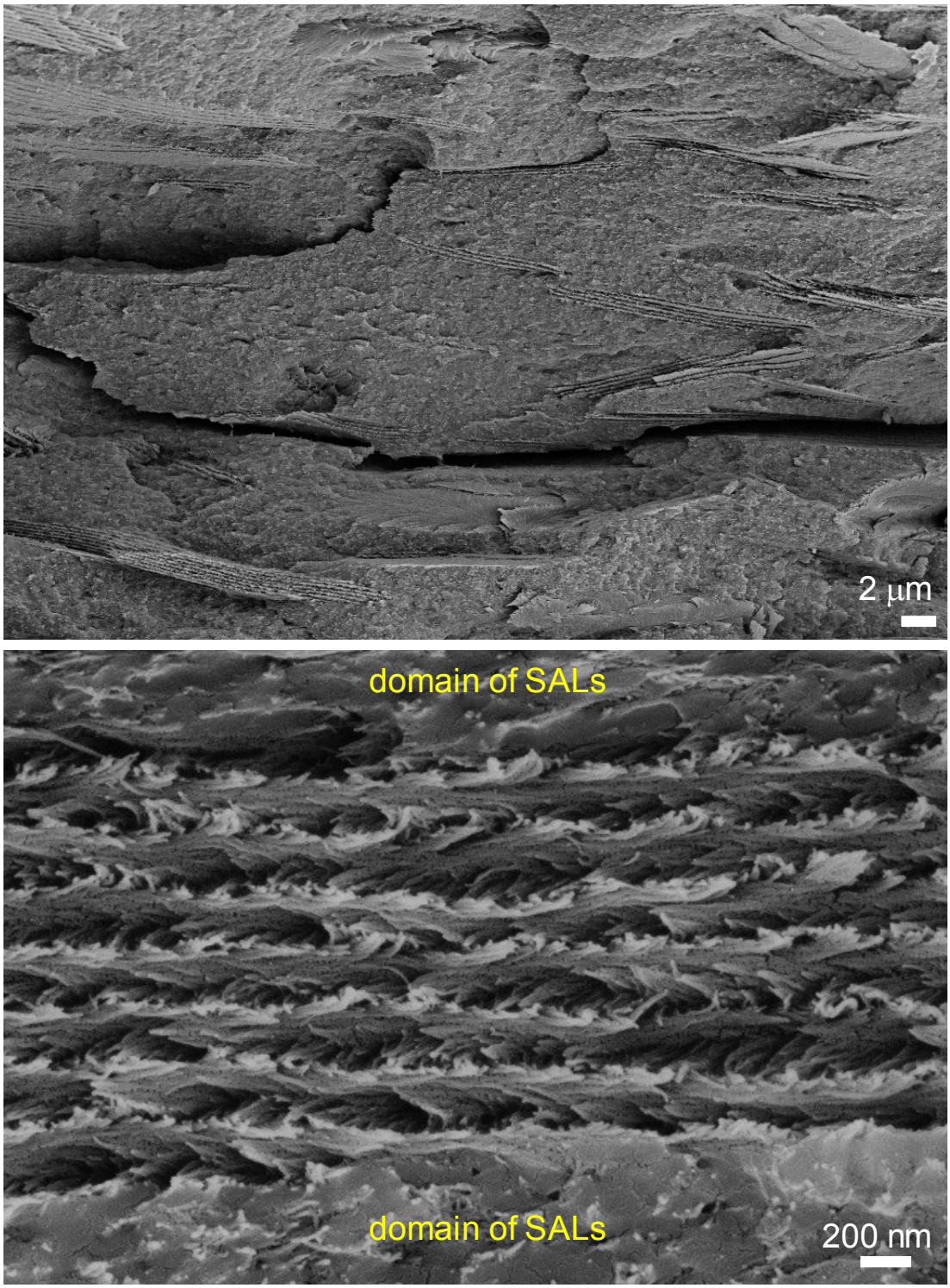

Fig. S9 SEM images at different magnifications of the fracture surface of $CF_{1.0}$.

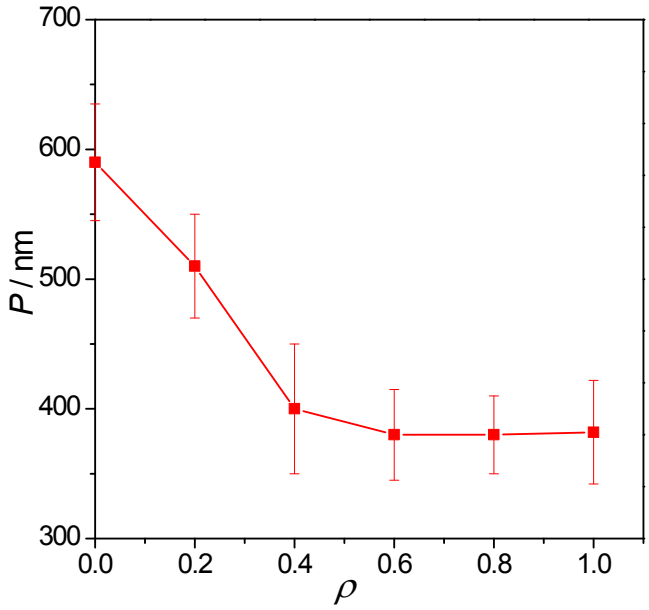

Fig. S10 Variation of P as a function of ρ derived from statistical analysis of the SEM images.

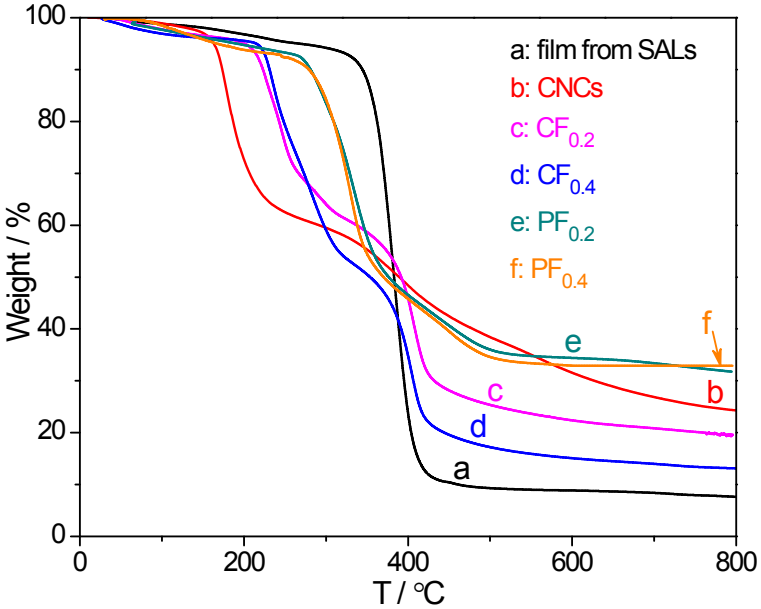

Fig. S11 TGA curves for different materials and films as indicated.

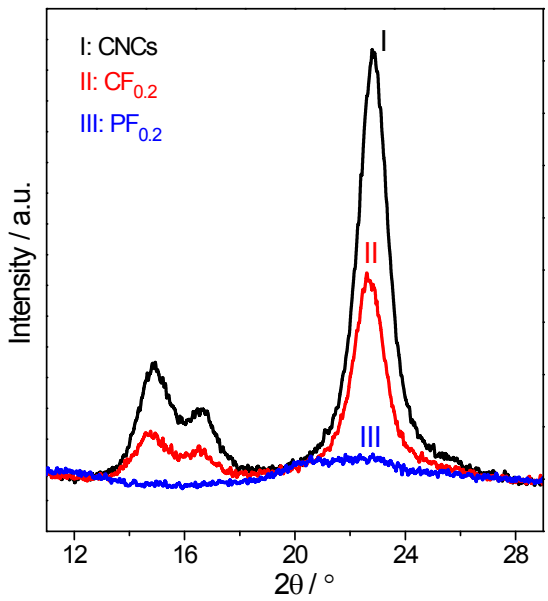

Fig. S12 XRD patterns of CNCs, $CF_{0.2}$ and $PF_{0.2}$.

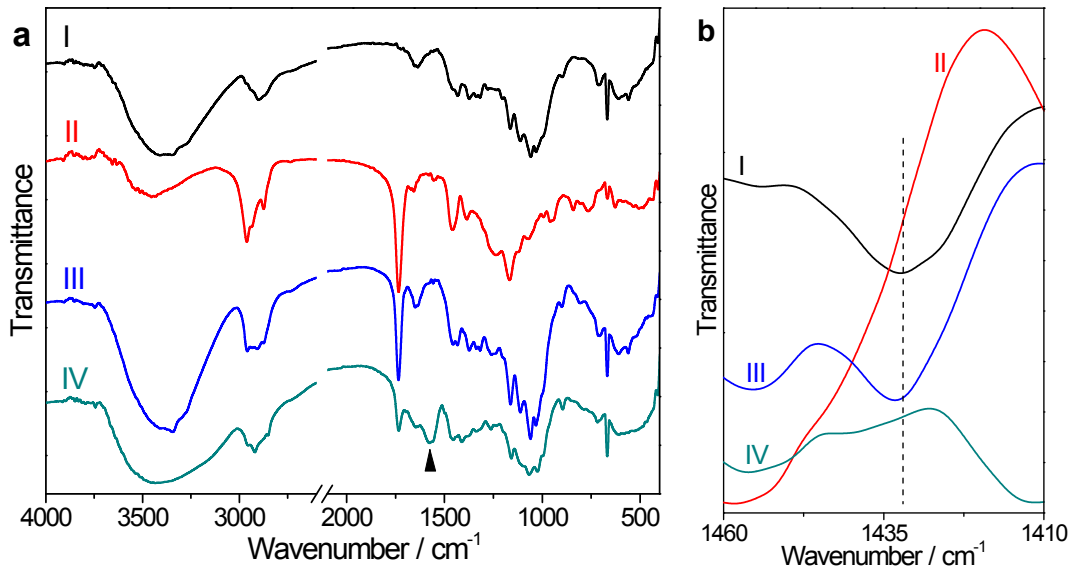

Fig. S13 FTIR spectra of CNCs (I), SALs (II), $CF_{0.2}$ (III) and $PF_{0.2}$ (IV), respectively. **a**) An overview. **b**) Magnified spectra in the region of 1460-1410 cm^{-1}. The dashed line in **b** is a guide for the eyes.

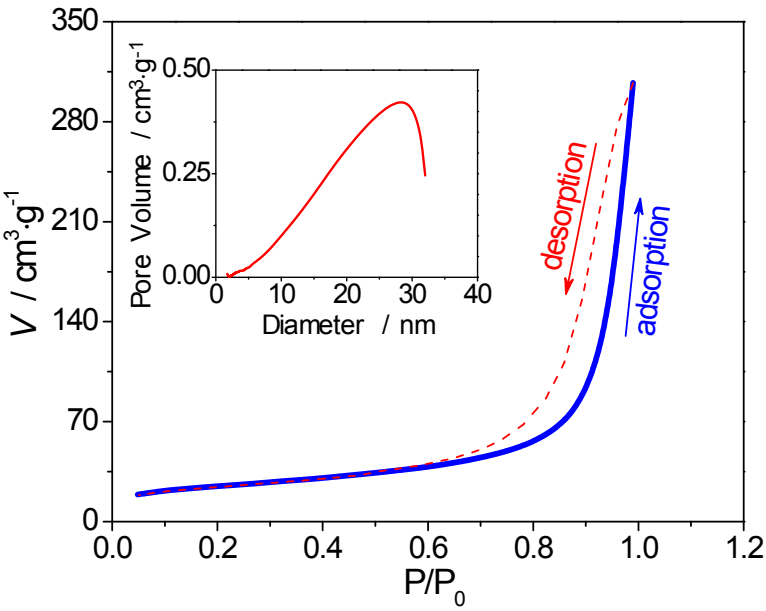

Fig. S14 N_2 adsorption/desorption isotherm of $PF_{0.2}$ prepared by $SCCO_2$-drying. The BJH pore size distribution is also shown inset.

Table S1 Changes in weight, size and volume from CFs to PFs.

	$CF_{0.2}$	$PF_{0.2}$	$CF_{0.4}$	$PF_{0.4}$
Weight / g	0.2012	0.0419	0.2458	0.0865
Thickness / mm	0.172	0.156	0.187	0.154
Diameter / mm	37	24.16	36	26.18
Volume Loss / %	-	61.3	-	56.4
Weight Loss / %	-	79.2	-	64.8

Table S2. The polarity, refractive index (n_D) and viscosity of MeOH, EtOH, ProOH as well as H_2O.

	polarity	n_D	viscosity
H_2O	10.2	1.3330	1
MeOH	6.6	1.3284	0.6
EtOH	4.3	1.3614	1.2
ProOH	4	1.3862	2.27

Notion:

Besides the influence of the solvent polarity as discussed in the maintext, we have also simply analyzed the possible influence caused by the change of n_D. As the films are dried under the same condition, solvent with a higher viscosity has more chance to be trapped inside the film, which will induce a change of n_D. This effect is enhanced considering that solvent with a higher viscosity also exhibits a higher n_D, as seen from the table above.

Although such analysis is qualitatively correct for the series of films prepared from MeOH, EtOH and ProOH, difficulties were encountered when generalized to the film prepared from H_2O. Thus we conclude that, the influence of the change of n_D, if it does exist, should be minor.